Contents

This page intentionally left blank

God does not care about our mathematical difficulties; He integrates empirically.

Albert Einstein, quoted by Leopold Infeld in *Quest: an autobiography*, 1941

Chapter 6

Discussion

TODO: introductory paragraph

6.1 Preventing coarse model instability

One of the earliest issues encountered in this work was the potential for low-resolution models to become numerically unstable, making it difficult to obtain a baseline for evaluating parametrised models. Aside from the need for a baseline, it seems unlikely that a simple parametrisation scheme like the one developed in Chapter 4 would have improved the skill of a coarse model on the brink of instability. Since this work was not concerned with accurately representing physical reality, I chose to artificially add hyperviscosity terms to the equations. Another option for future work could be to use stress-free boundary conditions on the top and bottom plates (i.e., $w(z = 0, 1) = \partial u/\partial z|_{z=0,1} = 0$) rather than the no-slip condition. This could reduce the large near-wall temperature and velocity gradients that often triggered instability at low resolutions.

However, when modelling real-world systems such as the atmosphere, one does not have the freedom to simply alter the governing equations. Successful data-driven parametrisation in these cases will depend on the careful choice of the numerical methods used to discretise and solve the equations such that the underlying coarse model is stable, even if it is inaccurate. Futher work with the Rayleigh-Bénard system should investigate whether other types of solvers (finite difference/volume/element, etc.) are more suitable.

6.2 The coarse-graining problem

TODO: move to conclusion

The predictability of the subgrid tendencies was found to depend strongly on the method used to coarse-grain the high-resolution solutions, and the development of an an appropriate method was non-trivial. These findings can be justified with further discussion.

The Lorenz '96 system (2.1) explicitly separates its degrees of freedom into "coarse" and "fine" variables, allowing one to unambiguously define a reduced model by simply truncating the fine variables from the full model. The corresponding "coarse-graining" operation is trivial: just discard the fine variables. For spatially continuous systems like Rayleigh-Bénard, however, standard practice is to construct high- and low-resolution models independently from each other by applying (possibly different) discretisation schemes to the governing equations. Since the low-resolution model is not, in general, obtained by explicitly truncating the high-resolution model, it is up to the modeller to choose a coarse-graining

operation that maps the high-resolution state space to the low-resolution one. While instructive, Lorenz '96 and its coarse/fine paradigm are not helpful analogues in this respect.

6.3 Strategies for improving subgrid tendency prediction

Another obstacle to data-driven parametrisation for spatially continuous problems is that there is a very large number of possible subgrid tendency predictors. For Rayleigh-Bénard, one not only has the three prognostic variables, but also their derivatives to arbitrary order in the two spatial directions. The position-dependence of the subgrid tendency statistics was a further complication, adding z to the list of predictors. One could even use spatially or temporally nonlocal predictors (i.e., the values of the variables at nearby points in space or previous time steps)—a possibility that was not even considered in this work. It would be impossible for a human to explore every possible combination. Supervised machine learning algorithms, discussed briefly in § 1.3.2, are much better-suited to regression problems with large numbers of predictors and could potentially capture hidden and/or nonlinear relationships between these predictors and the subgrid tendencies. There is no doubt, however, that this work was limited by the simplicity of the predictors and regression models that were considered, and future work using more sophisticated statistical models may indeed have greater success without needing to resort to machine learning.

This work was further limited by its use of purely deterministic parametrisation schemes despite the existence of considerable residuals in the subgrid tendency regressions Figures 4.8–4.10. Stochastic parametrisation, discussed in § 1.3.1, has the potential to reduce mean-state model biases by emulating the observed residuals. With the tools I have developed for the Rayleigh-Bénard problem, it would be relatively straightforward to experiment with various stochastic perturbations of the existing deterministic scheme (4.4), beginning with those that have been tested for Lorenz '96 (see § 2.2). This would include the use of time-correlated (e.g., AR(1)) noise to reflect the persistence (memory) of the subgrid tendencies.

6.4 Physical explanation of subgrid tendency correlations

Despite the difficulties described in § 6.3, the joint histograms in Chapter 4 gave clear evidence of subgrid tendency predictability in the near-wall regions. In this section, I argue that (at least) the correlations involving the θ subgrid tendency can be physically explained and are not spurious. As a reminder, the results in question are:

1. The negative correlation between the θ subgrid tendency and w near $z = 0, 1$,
2. The positive correlation between the θ subgrid tendency and $\partial u/\partial x$ near $z = 0$ and the negative correlation near $z = 1$, and
3. The negative correlation between the θ subgrid tendency and the θ tendency predicted by the coarse model, near $z = 0, 1$.

I attribute these to the coarse-graining step, which, in the process of smoothing the temperature field, widens the thermal boundary layer considerably (compare Figure 4.2a to Figure 4.2c). On the one hand, there is little change in boundary layer thickness between the coarse state at time t and the true coarse state at time $t + \delta t$ because the latter is obtained by first applying the fine model to the fine state at time t (Step 1) and then coarse-graining (Step 2). This means that the true coarse tendencies (Step 4) are close to zero in the boundary layers. On the other hand, the coarse model prediction for time $t + \Delta t$ is obtained by first coarse-graining the fine state at time t (Step 2) and *then* applying the coarse model (Step 3). At the high Rayleigh number used here ($\mathrm{Ra} = 10^9$), advection in the coarse model immediately begins to thin out the unusually thick boundary layers.

Figure 6.1 gives a cartoon illustration of the effect of advection on the temperature field. Consider the bottom left green dot, which is located near the lower wall, at the base of a rising convection plume. At this point, the vertical velocity w is positive, and fluid is rushing inwards from the left and right, making $\partial u/\partial x$ negative. The aforementioned widening of the thermal boundary layer by the coarse-graining operation has effectively created a large mass of warmer fluid beneath; this is advected upwards in the coarse model, meaning that the coarse model predicts a positive tendency $\partial\theta/\partial t$ at the green dot. As explained in the previous paragraph, the true value of $\partial\theta/\partial t$ is closer to zero at this point. The subgrid tendency—the true tendency minus predicted tendency—is therefore negative.

Applying the same logic to the other three green dots in Figure 6.1, as shown by the text boxes, one finds that the signs of w and the predicted tendency are always opposite to the sign of the subgrid tendency. The conclusion is that these variables must be negatively correlated with the subgrid tendency near $z = 0, 1$. On the other hand, the $\partial u/\partial x$ has the same sign as the subgrid tendency near $z = 0$ (i.e., positive correlation) and the opposite sign near $z = 1$ (i.e., negative correlation). These predictions are all consistent with the observations in Chapter 4.

It is farily easy to attribute the subgrid θ tendency correlations to advection in the coarse model because θ behaves a tracer that is nearly conserved by the flow. The velocity field, however, also has a boundary layer that is widened by the coarse-graining operation, leading me to conjecture that the subgrid u and w tendency correlations can be explained using a similar argument. The fact that all the correlations exhibit similar height dependence lends credence to the conjecture. If this is true, then the fact that θ is more closely conserved by the flow than u or w could explain why the correlations for θ were observed to be consistenly stronger than the other variables (see, e.g., Table 4.2).

While it is not surprising that the subgrid tendency statistics are height-dependent, it is interesting that this work was unable to produce evidence of predictability in the interior of the domain, away from $z = 0, 1$. Future work should investigate whether more advanced statistical models and/or machine learning are able to reveal correlations in this region.

6.5 Unanswered questions

6.6 Conclusion

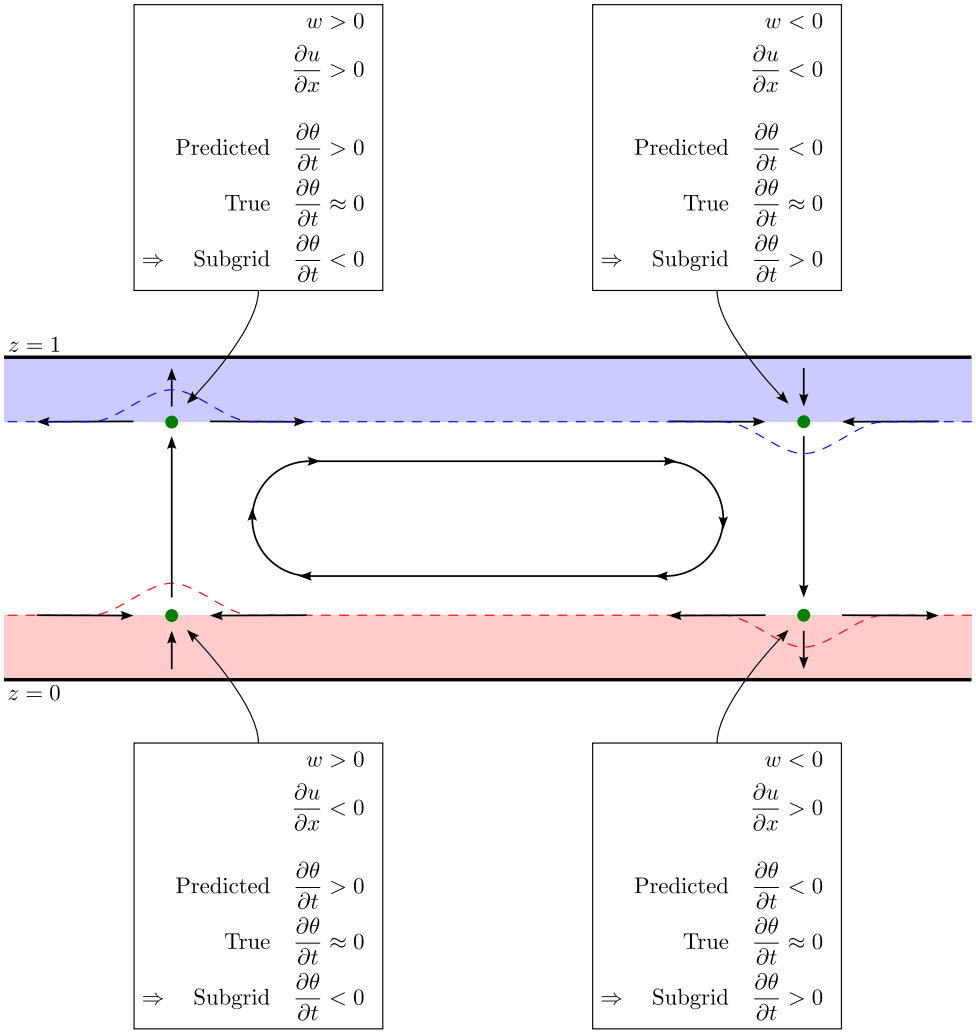

Figure 6.1: Cartoon illustration of the effect of advection on the coarse-grained temperature field when it is evolved using the coarse model. Thick horizontal black lines represent the top and bottom domain walls. Black arrows represent the velocity field. The warm and cold thermal boundary layers are indicated by red and blue shading respectively. Advection deforms the isotherms in the boundary layer, which are initially approximately flat, in the manner indicated by the dashed red and blue lines. The text boxes list the signs of the predictors and predictands at the four green dots, demonstrating the claimed correlations.